

Output spectrum of a measuring device at arbitrary voltage and temperature

A. SHNIRMAN¹, D. MOZYRSKY² and I. MARTIN²

¹ *Institut für Theor. Festkörperphysik, Uni. Karlsruhe, D-76128 Karlsruhe, Germany.*

² *Theoretical Division, Los Alamos National Laboratory, Los Alamos, NM 87545, USA.*

PACS. 74.50.+r – Tunneling phenomena; point contacts, weak links, Josephson effects.

PACS. 03.65.Ta – Foundations of quantum mechanics; measurement theory.

Abstract. – We calculate the noise spectrum of the electrical current in a quantum point contact which is used for continuous measurements of a two-level system (qubit). We generalize the previous results obtained for the regime of high transport voltages (when V is much larger than the qubit's energy level splitting B (we put $e = \hbar = 1$)) to the case of arbitrary voltages and temperatures. When $V \sim B$ the background output spectrum is essentially asymmetric in frequency, i.e., it is no longer classical. Yet, the spectrum of the amplified signal, i.e., the two coherent peaks at $\omega = \pm B$ is still symmetric. In the emission (negative frequency) part of the spectrum the coherent peak can be 8 times higher than the background pedestal. Alternatively, this ratio can be seen in the directly measureable *excess* noise. For $V < B$ and $T = 0$ the coherent peaks do not appear at all. We relate these results to the properties of linear amplifiers.

Introduction. – For quantum information technology it is necessary to investigate properties of real physical systems used as quantum detectors. Certain quantum algorithms require an efficient (single-shot) read out the final state of a qubit. This can be done by either strongly coupled threshold detectors (see e.g., Refs. [1,2]), or by “measurement in stages” strategy [3]. For weakly coupled detectors the only way to perform single-shot measurements is to be in the quantum-non-demolition (QND) regime, i.e., by measuring an observable which commutes with the Hamiltonian and is, thus, conserved. In the solid state domain this regime has been investigated in, e.g., Refs. [4–6].

In this letter we concentrate on continuous weak non-QND measurements (monitoring) of the coherent oscillations of a qubit (two-level system, spin-1/2). This regime was the main focus of Refs. [7–10]. It is realized, e.g., for the transverse coupling between the spin and the meter, e.g., when the effective magnetic field acting on the spin is along the x -axis while σ_z is being measured. In this case one observes the stationary state properties of the system, after the information about the initial state of the qubit is lost. Thus, this regime is not useful for quantum computation. Yet, studying the properties of the meter in the stationary monitoring regime, one can obtain information necessary in order to, later, employ the meter in the QND regime. Another motivation for our study comes from the recent activity in the STM single spin detection (see, e.g., Ref. [11,12]).

Without monitoring and without coupling to other sources of dissipation the observable σ_z would show coherent (Larmor) oscillations. When subject to monitoring these oscillations give rise to a peak in the output spectrum of the meter at the Larmor frequency. The laws of quantum mechanics limit the possible height of the peak. In the case of a 100% efficient (quantum limited) detector and when all the noises are white on the frequency scale B the peak can be only 4 times higher than the background noise pedestal [7]. Inefficiency of the detector reduces the height of the peak further.

Usually the analysis of the continuous measurements in voltage driven meters is limited to the case $V \gg B$ [4, 7, 8]. The output noise spectrum in this regime is almost symmetric (classical) at frequencies of order and smaller than B . In this letter we remove the restriction $V \gg B$. At low voltages, $V \sim B$, the output noise is essentially asymmetric, i.e., the output signal is quantum. In other words, we have to differentiate between the absorption ($\omega > 0$) and the emission ($\omega < 0$) spectra of the detector (see, e.g. Ref. [13]). We show, however, that the qubit's contribution to the full output noise as well as to the experimentally accessible *excess* noise is symmetric. We calculate this contribution for arbitrary voltage and temperature. In the excess noise, which is obtained by subtracting the equilibrium detector noise ($V = 0$) from the output at $V \neq 0$, the peak to background ratio can reach 8 for $V \sim B$.

General considerations. – We start from the general theory of linear amplifiers [5, 6, 9, 14] which applies in the regime of weak continuous monitoring. The Hamiltonian of the whole system including the amplifier (meter) reads $H = H_{\text{meter}} + H_{\text{qs}} + c\sigma Q$, where σ is the measured observable of the small quantum system governed by H_{qs} , Q is the input variable of the amplifier governed by H_{meter} , and c is the coupling constant. The meter is necessarily driven out of equilibrium. We study the output variable of the meter I . The stationary average value $\langle I \rangle$ is only slightly changed by the presence of the qubit. Much more interesting is the spectrum of fluctuations $\langle \delta I_\omega^2 \rangle \equiv \int dt \langle \delta I(t) \delta I(0) \rangle e^{i\omega t}$. While it is convenient to discuss physics in terms of the symmetrized $S_I(\omega) \equiv (1/2)[\langle \delta I_\omega^2 \rangle + \langle \delta I_{-\omega}^2 \rangle]$ and anti-symmetrized $A_I(\omega) \equiv (1/2)[\langle \delta I_\omega^2 \rangle - \langle \delta I_{-\omega}^2 \rangle]$ correlators, the calculations are more convenient in terms of the Keldysh-time-ordered Green's functions (see, e.g., Ref. [15]). Thus we define $G_I(t, t') = -i\langle T_K \delta I(t) \delta I(t') \rangle$. This is a 2×2 matrix as both t and t' can belong either to the forward or to the backward Keldysh contours [15]. We have the two basic components $iG_I^>(t - t') = \langle \delta I(t) \delta I(t') \rangle$ and $iG_I^<(t - t') = \langle \delta I(t') \delta I(t) \rangle$ from which all others are built. The retarded and advanced components are defined as $G_I^R(t - t') = \theta(t' - t)[G_I^>(t - t') - G_I^<(t - t')]$ and $G_I^A(t - t') = -\theta(t - t')[G_I^>(t - t') - G_I^<(t - t')]$. These two components describe, usually, the response of I to a perturbation coupled to I . The Keldysh component defined as $G_I^K(t - t') = G_I^>(t - t') + G_I^<(t - t')$ is related to the symmetrized correlator. It is easy to obtain the following relations: $iG_I^R(\omega) - iG_I^A(\omega) = 2A_I(\omega)$ and $iG_I^K(\omega) = 2S_I(\omega)$. We will also need $G_{IQ}(t, t') \equiv -i\langle T_K \delta I(t) \delta Q(t') \rangle$, $G_{QI}(t, t') \equiv -i\langle T_K \delta Q(t) \delta I(t') \rangle$, and $\Pi(t, t') \equiv -i\langle T_K \delta \sigma(\tau) \delta \sigma(\tau') \rangle$. Various components of these Green's functions are defined analogously to those of G_I .

We assume that one is allowed to use Wick's theorem for the operators I , Q , and σ . Frequently, even if Wick's theorem does not apply, one can still use it for the lowest (in the coupling constant) calculations and show that the corrections are of the higher order. We return to this subject later. Since the dynamics of the measured system changes substantially as a result of measurement while the meter's one is perturbed weakly, we use the full ("thick") Green's function Π , while for G_{IQ} and G_{QI} one keeps the unperturbed values. Then the lowest order irreducible correction to the Green's function $G_I(t, t')$ reads

$$\delta G_I(t, t') = c^2 \oint \oint d\tau d\tau' G_{IQ}(t, \tau) \Pi(\tau, \tau') G_{QI}(\tau', t'). \quad (1)$$

In the stationary regime this gives

$$\delta G_I(\omega) = c^2 \begin{pmatrix} G_{IQ}^R(\omega) & G_{IQ}^K(\omega) \\ 0 & G_{IQ}^A(\omega) \end{pmatrix} \begin{pmatrix} \Pi^R(\omega) & \Pi^K(\omega) \\ 0 & \Pi^A(\omega) \end{pmatrix} \begin{pmatrix} G_{QI}^R(\omega) & G_{QI}^K(\omega) \\ 0 & G_{QI}^A(\omega) \end{pmatrix}. \quad (2)$$

For the Green's function G_{QI} we have $G_{QI}^R(\omega) = G_{IQ}^A(-\omega)$, $G_{QI}^A(\omega) = G_{IQ}^R(-\omega)$, and $G_{QI}^K(\omega) = G_{IQ}^K(-\omega)$. We introduce the notations $\lambda(\omega) = c G_{IQ}^R(\omega)$, $\lambda'(\omega) = c G_{QI}^R(\omega)$, where λ is the direct gain (amplification coefficient) of the amplifier, while λ' is the inverse gain. As $\lambda(t)$ and $\lambda'(t)$ are real, $\lambda(-\omega) = \lambda^*(\omega)$ and $\lambda'(-\omega) = \lambda'^*(\omega)$. Thus we obtain

$$\delta G_I^R(\omega) = \lambda(\omega) \lambda'(\omega) \Pi^R(\omega), \quad (3)$$

$$\delta G_I^K(\omega) = -2i \delta S_I(\omega) = |\lambda(\omega)|^2 \Pi^K(\omega) + 2ic \operatorname{Im} [\lambda(\omega) \Pi^R(\omega) G_{QI}^K(\omega)], \quad (4)$$

and $\delta G_I^A(\omega) = [\delta G_I^R(\omega)]^*$. We have also used $G_{QI}^K(\omega) = G_{IQ}^K(-\omega) = -[G_{IQ}^K(\omega)]^*$. The first term of (4) corresponds to the noise of the small system "amplified" by the meter. The second term is needed to fulfill the fluctuations-dissipation relation at equilibrium. We will see that it is also important at low voltages, i.e., when the detector is not driven far enough from equilibrium. For good amplifiers the inverse gain vanishes, $\lambda' = 0$, and we obtain $\delta G_I^R = 0$. Thus the contribution to the output correlator $\delta \langle \delta I_\omega^2 \rangle = i \delta G_I^> = (i/2)(\delta G_I^K + \delta G_I^R - \delta G_I^A) = (i/2)\delta G_I^K = \delta S_I(\omega)$ is symmetric in frequency, i.e., $\delta A_I(\omega) = 0$. Vanishing of λ' also means that further amplifiers using I as an input will not add to the back-action.

Spin's dynamics. – When an observable of a qubit (a component of spin-1/2) is being measured we can assume without loss of generality $\sigma = \sigma_z$. The spin is subject to an (effective) magnetic field \vec{B} , i.e., $H_{qs} = -(1/2)\vec{B} \cdot \vec{\sigma}$. Its dynamics is, thus, obtained from the Hamiltonian

$$H = -\frac{1}{2} \vec{B} \cdot \vec{\sigma} - \frac{1}{2} Q \sigma_z, \quad (5)$$

where we have put $c = -1/2$ so that Q can be interpreted as fluctuating magnetic field. We exclude the case $\vec{B} \parallel \mathbf{z}$, in which the measured observable $\sigma = \sigma_z$ commutes with the Hamiltonian and, thus, is conserved. This regime is known as the quantum-non-demolition (QND) one and has been treated, e.g., in Refs. [4–6]. In all other cases the stationary state is reached after some transient period and we can study the output spectrum of the meter.

For simplicity we assume no extra dissipation sources acting on the qubit except for the meter. The spin's Green functions (correlators) are obtained within the standard Bloch-Redfield approach [16, 17] which is applicable as long as the dissipation is weak (see below). Within this approach one, first, calculates the markovian evolution operator for the spin's density matrix, and, then, uses the "quantum regression theorem" [13] to obtain the correlators. For this lowest order perturbative (in the spin-meter coupling) calculation one only needs to know the (unperturbed by the spin) fluctuations spectrum, $\langle Q_\omega^2 \rangle$. One, then, obtains

$$\begin{aligned} \Pi^K(\omega) &= -i \sin^2 \theta \left[\frac{2\Gamma_2}{(\omega - B)^2 + \Gamma_2^2} + \frac{2\Gamma_2}{(\omega + B)^2 + \Gamma_2^2} \right] - i \cos^2 \theta \frac{4\Gamma_1}{\omega^2 + \Gamma_1^2} [1 - \langle \sigma_{\vec{B}} \rangle^2], \\ \Pi^R(\omega) &= \sin^2 \theta \langle \sigma_{\vec{B}} \rangle \left[\frac{1}{\omega - B + i\Gamma_2} - \frac{1}{\omega + B + i\Gamma_2} \right], \end{aligned} \quad (6)$$

where θ is the angle between \vec{B} and \mathbf{z} . The stationary spin polarization along \vec{B} is given by $\langle \sigma_{\vec{B}} \rangle = h(B)$, where $h(\omega) \equiv A_Q(\omega)/S_Q(\omega)$, while $S_Q(\omega) \equiv (1/2)[\langle Q_\omega^2 \rangle + \langle Q_{-\omega}^2 \rangle]$ and

$A_Q(\omega) \equiv (1/2)[\langle Q_\omega^2 \rangle - \langle Q_{-\omega}^2 \rangle]$. The relaxation (Γ_1) and the dephasing (Γ_2) rates are given by:

$$\Gamma_1 = (1/2) \sin^2 \theta S_Q(\omega = B) \quad , \quad \Gamma_2 = (1/2) \Gamma_1 + (1/2) \cos^2 \theta S_Q(\omega = 0) . \quad (7)$$

The applicability condition of the Bloch-Redfield approach is $\Gamma_1, \Gamma_2, \delta B \ll B$, where δB is the renormalization of the energy splitting (Lamb shift). If one treats the Lorentzians in (6) as true delta functions, one can derive from the second equation of (6) a relation resembling the fluctuation-dissipation theorem: $\Pi^R(\omega) - \Pi^A(\omega) \approx h(\omega) \Pi^K(\omega)$. Note, that, although we use the “diagrammatic” language of Keldysh Green functions, Eqs. (6) are obtained without any diagrams or assumptions about the applicability of Wick’s theorem.

Spin’s contribution to the output spectrum. – Substituting Eqs. (6) into Eq. (4) we obtain spin’s contribution to the symmetrized output spectrum of the meter:

$$\begin{aligned} \delta S_I(\omega > 0) = & \sin^2 \theta \left[\frac{\Gamma_2}{(\omega - B)^2 + \Gamma_2^2} \right] \left\{ |\lambda(\omega)|^2 - \frac{h(B)}{2} \text{Re} [\lambda(\omega) G_{QI}^K(\omega)] \right\} \\ & + \sin^2 \theta \left[\frac{\omega - B}{(\omega - B)^2 + \Gamma_2^2} \right] \frac{h(B)}{2} \text{Im} [\lambda(\omega) G_{QI}^K(\omega)] \\ & + \cos^2 \theta \frac{2\Gamma_1}{\omega^2 + \Gamma_1^2} [1 - h^2(B)] |\lambda(\omega)|^2 . \end{aligned} \quad (8)$$

We assume that $\lambda(\omega)$ and $G_{QI}^K(\omega)$ are smooth near $\omega = \pm B$ and $\omega = 0$. Then, the first term of (8) gives two peaks near $\omega = \pm B$ with width Γ_2 . The third term gives a peak at $\omega = 0$ with width Γ_1 . The second term of (8) gives the Fano shaped contributions near $\omega = \pm B$. The simplest situation arises when $\theta = \pi/2$ and $h(B) \rightarrow 0$ (at very high transport voltages the effective temperature of the spin is infinite and $\langle \sigma_{\vec{B}} \rangle \rightarrow 0$). Then only the peaks at $\omega = \pm B$ survive with the height $\delta S_I(B) = |\lambda(B)|^2 / \Gamma_2 = 4|\lambda(B)|^2 / S_Q(B)$. The peak to pedestal ratio $\delta S_I(B) / S_I(B) = 4|\lambda(B)|^2 / (S_Q(B) S_I(B))$ was shown [7–10] to be limited by 4. Below we investigate the coherent peaks at arbitrary voltage and temperature for a specific example of a meter with the purpose to explore the effect of the rest of the terms in (8).

Quantum Point Contact (QPC) as a meter. – The QPC devices are known to serve as effective meters of charge (see, e.g., Refs. [18–21]). The conductance of the QPC is controlled by the quantum state of a qubit. We focus on the simplest limit of a tunnel junction when the transmissions of all the transport channels are much smaller than unity. This model has previously been used by many authors [22–24]. It also corresponds to the model considered in Ref. [12] in the regime of lead electrons fully polarized along the z axis, $\mathbf{m}_R = \mathbf{m}_L = \mathbf{z}$. The tunnel junction limit is described by the following Hamiltonian

$$H = \sum_l \epsilon_l c_l^\dagger c_l + \sum_r \epsilon_r c_r^\dagger c_r + \sum_{l,r} (t_0 + t_1 \sigma_z) (c_r^\dagger c_l + h.c.) - (1/2) \vec{B} \vec{\sigma} . \quad (9)$$

The transmission amplitudes t_0 and t_1 are assumed to be real positive and small (tunnel junction limit). We also assume $t_1 \ll t_0$ to be in the linear amplifier regime.

For brevity we introduce the operator $X \equiv \sum_{l,r} c_l^\dagger c_r$ and then $j \equiv i(X - X^\dagger)$ and $q \equiv (X + X^\dagger)$. The current operator is given by $I = (t_0 + t_1 \sigma_z) j$, while the tunneling Hamiltonian is $H_T = (t_0 + t_1 \sigma_z) q$. We see that the analysis of the amplifiers presented above cannot be directly applied. First, the interaction term between the spin and the QPC, i.e., $t_1 q \sigma_z$ (thus, in our case $Q = -2t_1 q$), is not the full interaction vertex but rather a part of H_T . Second, the current operator I contains the spin’s operator σ_z explicitly. One possible way to resolve these

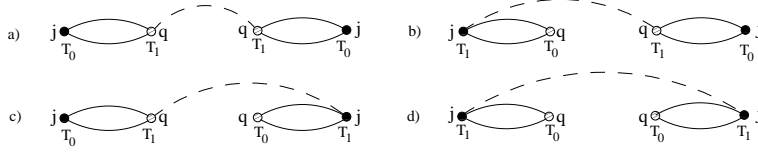


Fig. 1 – The diagrams leading to Eq. (13). The loops represent the Green functions G_{jq} and G_{qj} . Each of these Green's functions is actually a combination of two electronic ones (solid lines). The dashed line is the spin's Green function.

difficulties (see e.g., [7,9]) is to include the spin-independent part of H_T , namely $t_0 q$, into the zeroth-order Hamiltonian. This amounts to working in the basis of scattering states. Here we adopt a simpler procedure suitable for QPC's in the tunneling regime. We expand in the full H_T and keep all the terms up to the order $t_0^2 t_1^2$. For this we need the following zeroth-order Green's functions: $G_{qq} \equiv -i\langle T_K q(t)q(t') \rangle$, $G_{jj} \equiv -i\langle T_K j(t)j(t') \rangle$, and $G_{jq} \equiv -i\langle T_K j(t)q(t') \rangle$, $G_{qj} \equiv -i\langle T_K q(t)j(t') \rangle$. For $\omega \ll D$, where D is the electronic bandwidth (the Fermi energy) we obtain

$$G_{qq}(\omega) = G_{jj}(\omega) = -i\eta \begin{pmatrix} \omega + i... & 2s(\omega) \\ 0 & -\omega + i... \end{pmatrix}, \quad (10)$$

$$G_{jq}(\omega) = -G_{qj}(\omega) = \eta \begin{pmatrix} V(1 + iO(\omega/D)) & 2a(\omega) \\ 0 & -V(1 - iO(\omega/D)) \end{pmatrix}, \quad (11)$$

where $\eta \equiv 2\pi\rho_L\rho_R$. We have also introduced the two following functions:

$$s/a(\omega) \equiv \frac{V+\omega}{2} \coth \frac{V+\omega}{2T} \pm \frac{V-\omega}{2} \coth \frac{V-\omega}{2T}. \quad (12)$$

In Eq. (10) ... stand for the real part of the retarded (advanced) components. The factors $1 \pm iO(\omega/D)$ in (11) are responsible for making the functions $G_{jq}^R(t)$ and $G_{jq}^A(t)$ causal. As we are interested in the low frequencies ($\omega \ll D$) we approximate those factors by 1.

Peaks in the output noise spectrum. – We combine the Green functions $G_{jq}(\omega)$, $G_{qj}(\omega)$, and $\Pi(\omega)$ (see Eq. 6) into diagrams to calculate the qubit's contribution to the current-current Green function δG_I . The Wick theorem does not apply to the spin operators. However, using the Majorana representation of the spin operators and recently proved useful identities (see Refs. [25,26]) we are able to show that in order $t_0^2 t_1^2$ the answer is given by the diagrams shown in Fig. 1. We obtain $\delta G_I = t_0^2 t_1^2 [G_{jq}(\omega) + G_{jq}^A(0) \cdot \hat{1}] \Pi(\omega) [G_{qj}(\omega) + G_{qj}^A(0) \cdot \hat{1}]$, which can be rewritten as

$$\delta G_I = (1/\pi^2) g_0 g_1 \begin{pmatrix} V & a(\omega) \\ 0 & 0 \end{pmatrix} \begin{pmatrix} \Pi^R & \Pi^K \\ 0 & \Pi^A \end{pmatrix} \begin{pmatrix} 0 & -a(\omega) \\ 0 & V \end{pmatrix}, \quad (13)$$

where we have defined the conductances as $g_0 \equiv 2\pi\eta t_0^2$ and $g_1 \equiv 2\pi\eta t_1^2$. It is worth comparing Eqs. (13) and (2). Even though the simple formalism leading to Eq. (2) was not directly applicable in our case, the result (13) looks very similar. We can interpret, therefore, $\lambda = (1/\pi) \sqrt{g_0 g_1} V$, $\lambda' = 0$, and $cG_{IQ}^K(\omega) = (1/\pi) \sqrt{g_0 g_1} a(\omega)$. Thus the tunnel barrier possesses the property $\lambda' = 0$ at all frequencies. This assures that $\delta G_I^{R/A} = 0$ and the contribution to the current-current correlator is symmetric:

$$\begin{aligned} \delta S_I(\omega > 0) &= (1/\pi^2) g_0 g_1 V^2 \sin^2 \theta \frac{\Gamma_2}{(\omega - B)^2 + \Gamma_2^2} \left[1 - \frac{a(\omega)h(B)}{V} \right] \\ &+ (1/\pi^2) g_0 g_1 V^2 \cos^2 \theta \frac{2\Gamma_1}{\omega^2 + \Gamma_1^2} [1 - h^2(B)]. \end{aligned} \quad (14)$$

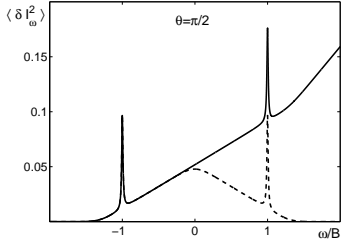


Fig. 2

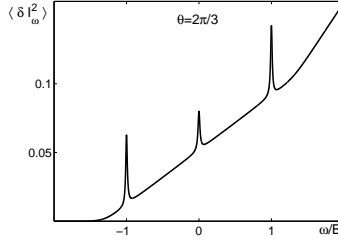


Fig. 3

Fig. 2 – Output noise power for $\theta = \pi/2$, $g_0 = 0.25$, $g_1 = 0.05$, $T = 0.05B$, and $V = 1.3B$. Solid line: the full correlator; dashed line: the excess spectrum.

Fig. 3 – Same parameters but $\theta = 2\pi/3$. Only the full correlator shown.

We note that in our example $S_Q(\omega) = 2it_1^2 G_{qq}^K(\omega) = (2/\pi) g_1 s(\omega)$ and $A_Q(\omega) = (2/\pi) g_1 \omega$. Then we obtain $h(B) = B/s(B)$, $\Gamma_1 = (1/\pi) g_1 \sin^2 \theta s(B)$, and $\Gamma_2 = (1/2\pi) g_1 \sin^2 \theta s(B) + (1/\pi) g_1 \cos^2 \theta s(0)$. Note, that no Fano shaped contributions appear due to the fact that both $\lambda(\omega)$ and $G_{IQ}^K(\omega)$ are real. The Lorentzians in Eq. (14) coincide with the ones obtained in Refs. [7–10]. The new result is the reduction factor for the peaks at $\omega = \pm B$ in the square brackets. This factor simplifies for $T = 0$. Then, if $V > B$, it is given by $(1 - B^2/V^2)$, while for $V < B$ it is equal to 0. In the last case the measuring device can not provide enough energy to excite the qubit and, therefore, the qubit remains in the ground state and does not produce any additional noise (see also Ref. [12]). The ratio between the peak's height and the pedestal's height is different for positive and negative frequencies. In the limit $g_1 \ll g_0$ we obtain $\langle \delta I_\omega^2 \rangle \approx it_0^2 G_{jj}^>(\omega) = (1/2\pi) g_0 (s(\omega) + \omega)$. Thus, for $T = 0$, and $B < V$ we obtain $\langle \delta I_{\pm B}^2 \rangle \approx (1/2\pi) g_0 V (1 \pm B/V)$ and $\delta \langle \delta I_{\pm B}^2 \rangle = \delta S_I(\pm B) \approx (2/\pi) g_0 V (1 - B^2/V^2)$ and

$$\frac{\delta \langle \delta I_{\pm B}^2 \rangle}{\langle \delta I_{\pm B}^2 \rangle} \approx 4(1 \mp \frac{B}{V}). \quad (15)$$

For $B \rightarrow V$ the ratio for the negative frequency peak reaches 8. In this limit, however, the peak's height is zero. For symmetrized spectra the maximal possible ratio is 4 (Ref. [8]). An interesting question is what exactly can be observed experimentally. If the further detection of the output noise is passive, like the photon counting in fluorescence experiments, one can only measure what the system emits, i.e. the noise at negative frequencies [27–29]. Moreover, in our example, the *excess* noise, i.e., $\langle \delta I_{\pm B}^2 \rangle(V) - \langle \delta I_{\pm B}^2 \rangle(V = 0)$, is symmetric. As shown in Ref. [30], if the excess noise is symmetric, it can be effectively measured even by a finite temperature LCR filter. In Figs. 2,3 we show examples of output noise spectrum and of the corresponding excess noise spectrum.

Conclusions. – We have calculated the output noise of the point contact used as a quantum detector of qubit's coherent oscillations for arbitrary voltage and temperature. In the regime $eV \sim B$ and $T \ll B$ the output noise is essentially asymmetric. Yet, the qubit's oscillations produce two symmetric peaks at $\omega = \pm B$ and also a peak at $\omega = 0$. Due to the vanishing of the inverse gain ($\lambda' = 0$) the peaks at $\omega = \pm B$ have equal height and, therefore, the negative frequency peak is much higher relative to its pedestal than the positive frequency one. The peak/pedestal ratio can reach 8. This can be observed by further passive detectors, which measure what the system emits, or by measuring the *excess* noise. The results of this paper are obtained for the simplest and somewhat artificial model of a quantum detector, a

QPC in the tunneling regime. It would be interesting to perform analogous calculations for more realistic detectors like SET's or QPC's with open channels (see e.g., Refs. [5, 29, 31]).

* * *

We thank Yu. Makhlin, Y. Levinson, and L. Bulaevskii for numerous fruitful discussions. A.S. was supported by the EU IST Project SQUBIT and by the CFN (DFG). D.M. and I.M. were supported by the U.S. DOE.

REFERENCES

- [1] D. Vion, A. Aassime, A. Cottet, P. Joyez, H. Pothier, C. Urbina, D. Esteve, and M. H. Devoret, *Science* **296**, 886 (2002).
- [2] I. Chiorescu, Y. Nakamura, C. J. P. M. Harmans, and J. E. Mooij, *Science* **299**, 1869 (2003).
- [3] O. Astafiev, Yu. A. Pashkin, T. Yamamoto, Y. Nakamura, and J. S. Tsai, *cond-mat/0402619* (2004).
- [4] A. Shnirman and G. Schön, *Phys. Rev. B* **57**, 15400 (1998).
- [5] A.A. Clerk, S.M. Girvin, and A.D. Stone, *Phys. Rev. B* **67**, 165324 (2003).
- [6] M. H. Devoret and R. J. Schoelkopf, *Nature* **406**, 1039 (2000).
- [7] A. N. Korotkov and D. V. Averin, *Phys. Rev. B* **64**, 165310 (2001).
- [8] A. N. Korotkov, *Phys. Rev. B* **63**, 085312 (2001).
- [9] D. V. Averin, In J. R. Friedman and S. Han, editors, *Exploring the Quantum-Classical Frontier* Commack, NY; cond-mat/0004364 (2002). Nova Science Publishers.
- [10] R. Ruskov and A. Korotkov, *Phys. Rev. B* **67**, 075303 (2003).
- [11] A. V. Balatsky and I. Martin, *cond-mat/0112407* (2001).
- [12] L. N. Bulaevskii, M. Hruška, and G. Ortiz, *Phys. Rev. B* **68**, 125415 (2003).
- [13] C. W. Gardiner and P. Zoller, *Quantum Noise*, Springer 2 edition (2000).
- [14] V. B. Braginsky and F. Ya. Khalili, *Quantum measurement*, Cambridge University Press Cambridge (1992).
- [15] J. Rammer and H. Smith, *Rev. Mod. Phys.* **58**, 323 (1986).
- [16] F. Bloch, *Phys. Rev.* **105**, 1206 (1957).
- [17] A. G. Redfield, *IBM J. Res. Dev.* **1**, 19 (1957).
- [18] M. Field, C. G. Smith, M. Pepper, D. A. Ritchie, J. E. F. Frost, G. A. C. Jones, and D. G. Hasko, *Phys. Rev. Lett.* **70**, 1311 (1993).
- [19] D. Sprinzak, Yang Ji, M. Heiblum, D. Mahalu, and H. Shtrikman, *Phys. Rev. Lett.* **88**, 176805 (2002).
- [20] E. Buks, R. Schuster, M. Heiblum, D. Mahalu, and V. Umansky, *Nature* **391**, 871 (1998).
- [21] J. M. Elzerman, R. Hanson, J. S. Greidanus, L. H. Willems van Beveren, S. De Franceschi, S. Tarucha L. M. K. Vandersypen, and L. P. Kouwenhoven, *cond-mat/0212489* (2002).
- [22] S. A. Gurvitz, *Phys. Rev. B* **56**, 15215 (1997).
- [23] A. N. Korotkov, *Phys. Rev. B* **60**, 5737 (1999).
- [24] H. S. Goan and G. J. Milburn, *Phys. Rev. B* **64**, 235307 (2001).
- [25] W. Mao, P. Coleman, C. Hooley, and D. Langreth, *Phys. Rev. Lett.* **91**, 207203 (2003).
- [26] A. Shnirman and Yu. Makhlin, *Phys. Rev. Lett.* **91**, 207204 (2003).
- [27] G. B. Lesovik and R. Loosen, *JETP Lett.* **65**, 295 (1997).
- [28] U. Gavish, Y. Levinson, and Y. Imry, *Phys. Rev. B* **62**, R10637 (2000).
- [29] R. Aguado and L. P. Kouwenhoven, *Phys. Rev. Lett.* **84**, 1986 (2000).
- [30] U. Gavish, Y. Imry, Y. Levinson, and B. Yurke, In Y.V. Nazarov and Y. Blanter, editors, *Quantum Noise in Mesoscopic Physics*. Kluwer (2003).
- [31] S. Pilgram and M. Büttiker, *Phys. Rev. Lett.* **89**, 200401 (2002).